cosmetics

MDPI

Article

Sustainable Valorization of Amazonian *Byrsonima crassifolia* (Murici): Phytochemical Profile and Antioxidant and Anti-Inflammatory Activities for Cosmetic Applications

Julia Amanda Rodrigues Fracasso [1], Fernando Yutaka de Ferreira [2], Luísa Taynara Silvério da Costa [1], Maria P. M. Marques [2], Ana Luísa Correia Brandão [2], Natalia Alves Zoppe [1], Kássia Aiko Asano-Miyashiro [1], Guilherme Justiniano-Mizumoto [3], João Tadeu Ribeiro-Paes [1], Valdecir Farias Ximenes [3] and Lucinéia dos Santos [1,*]

[1] Department of Biotechnology, School of Sciences and Languages, São Paulo State University (UNESP), Assis 19806-900, Brazil; j.fracasso@unesp.br (J.A.R.F.); na.zoppe@unesp.br (N.A.Z.)
[2] Molecular Physical-Chemistry R&D Unit, Department of Chemistry, University of Coimbra, 3004-535 Coimbra, Portugal; pmc@ci.uc.pt (M.P.M.M.); anabrandao@qui.uc.pt (A.L.C.B.)
[3] Department of Chemistry, School of Sciences, Bauru 17033-360, Brazil; guilherme.mizumoto@unesp.br (G.J.-M.); valdecir.ximenes@unesp.br (V.F.X.)
* Correspondence: lucineia.santos@unesp.br

Abstract

Considering the rich biodiversity of plant species in the Amazon region and the importance of investigating their medicinal properties as a means of valuing and preserving this biome, this study aimed to evaluate the phytochemical profile, cytotoxicity, and anti-inflammatory and antioxidant activities of the hydroalcoholic extract of *Byrsonima crassifolia* leaves (HEBC). Phytochemical analysis revealed high concentrations of phenols, with emphasis on condensed tannins. In addition, the presence of catechin, a precursor of condensed tannins, was analyzed and characterized by HPLC. The cytotoxic evaluation demonstrated the absence of cytotoxicity of HEBC at concentrations of 100, 200 and 400 µg/mL at all times analyzed. Finally, HEBC exhibited strong anti-inflammatory and antioxidant activities, likely associated with the presence of catechin. Therefore, with the aim of enhancing the value of *Byrsonima crassifolia* and promoting its sustainable use, HEBC emerges as a promising candidate for the development of a novel phytotherapeutic agent. In future studies, HEBC is intended to be incorporated into specific formulations and subjected to further analyses to confirm its therapeutic efficacy and safety.

Keywords: catechin; antioxidant; anti-inflammatory; *Byrsonima crassifolia*; HPLC; phytotherapeutic

Check for updates

Academic Editors: Maria Letizia Manca, Amparo Nacher, Matteo Perra, Ines Castangia and Mohamad Allaw

Received: 28 August 2025
Revised: 5 December 2025
Accepted: 12 December 2025
Published: 29 May 2026

Copyright: © 2026 by the authors. Licensee MDPI, Basel, Switzerland. This article is an open access article distributed under the terms and conditions of the Creative Commons Attribution (CC BY) license.

1. Introduction

Chronic skin inflammations, including atopic dermatitis, psoriasis, contact dermatitis, and cutaneous lupus erythematosus, are very common. Atopic dermatitis affects 15–20% of children and up to 10% of adults. Psoriasis impacts approximately 2–3% of the global population [1,2]. These conditions involve dysregulated immune activation and local oxidative stress, resulting in erythema, pruritus, desquamation, and impairment of the skin barrier, in addition to being associated with psychosocial impact and metabolic comorbidities [2]. Chronic inflammation and oxidative stress represent interdependent processes that sustain not only these dermatoses but also several systemic diseases, such as diabetes, cardiovascular disorders, and neurodegenerative conditions, through excessive production

of pro-inflammatory cytokines, accumulation of reactive oxygen species (ROS), and the formation of advanced glycation end-products (AGEs) [3].

Given the complexity of this pathophysiology, there is growing interest in plant extracts rich in secondary metabolites, particularly phenolic compounds, as bioactive ingredients in dermocosmetic formulations [4]. These compounds exhibit potent antioxidant and anti-inflammatory activities, modulating key molecular pathways involved in the cell aging process. Experimental evidence shows that such extracts can effectively neutralize reactive oxygen species (ROS), inhibit advanced glycation end-product (AGE) formation, and regulate the expression of pro-inflammatory mediators, thereby preserving cellular integrity and supporting skin health [5]. Furthermore, they generally present a favorable toxicological profile, with lower incidence of adverse effects and greater tolerability compared to conventional synthetic agents, highlighting the potential of phytochemicals as safe and effective adjuncts in skin care [6].

The Amazon region is notable for its incredible plant diversity, featuring species like *Byrsonima crassifolia*, commonly known as murici [7]. Although native to the Amazon, this plant has a distribution that extends from Mexico to Bolivia and Paraguay, being primarily present in Brazil's Northern Region, with secondary occurrences in the Northeast, Central-West, and Southeast regions [8]. Its traditional ethnopharmacological uses include diuretic, sedative, laxative, anti-inflammatory, and antifungal applications [9]. Furthermore, phytochemical studies have shown that different parts of the plant, including bark, branches, leaves, pulp, and seeds, contain phenolic compounds, flavonoids, tannins, and saponins, which contribute to its significant pharmacological potential [7].

Thus, given the close relationship between inflammation and oxidative stress, and the potential of the secondary metabolites present in murici, this study aimed to evaluate, using the hydroalcoholic extract of *Byrsonima crassifolia* leaves (HEBC), its in vitro anti-inflammatory and antioxidant properties. This investigation was motivated by the growing demand for effective complementary therapeutic alternatives with lower cytotoxicity compared to synthetic anti-inflammatory drugs commonly used in clinical practice. Accordingly, the present work sought to generate scientific evidence on the properties of the plant extract under study, highlighting its potential use as a complementary topical therapy for modulating the multifactorial processes associated with chronic cutaneous pathologies, while also opening perspectives for its future incorporation into cosmetic formulations.

2. Materials and Methods

2.1. Plant Material

The leaves were collected from seedlings cultivated at the Campus of the Faculty of Sciences and Letters–UNESP, in the city of Assis, São Paulo State. The species was identified as *Byrsonima crassifolia* by the Assis Herbarium of the University and deposited under voucher number 3169. The extraction process was carried out at the Laboratory of Pharmaceutical Technology in Phytoproducts (FITOTEC) at UNESP–Assis.

2.2. Preparation of the Extract of Byrsonima crassifolia (HEBC)

Initially, the *Byrsonima crassifolia* leaves were dried in a forced-air oven at 40 °C until constant weight. Then, the leaves were crushed in a mill. The hydroalcoholic extract was prepared at a ratio of 10 g of dried material per 100 mL of 70% ethanol in distilled water. The mixture was first agitated for 90 min and then subjected to static maceration protected from light for seven days. After this period, the extract was filtered; initially, the solution appeared brown, while the filtrate retained a greenish hue. The filtrate was then concentrated using a rotary evaporator at a controlled temperature of 70 °C to remove the solvent. During this process, the solution color shifted to a more brownish hue, likely

due to partial caramelization of sugars upon prolonged exposure to heat. Finally, the concentrated extract was dried in a forced-air oven at 40 °C until constant weight, resulting in a brownish-brown powder (Figure 1).

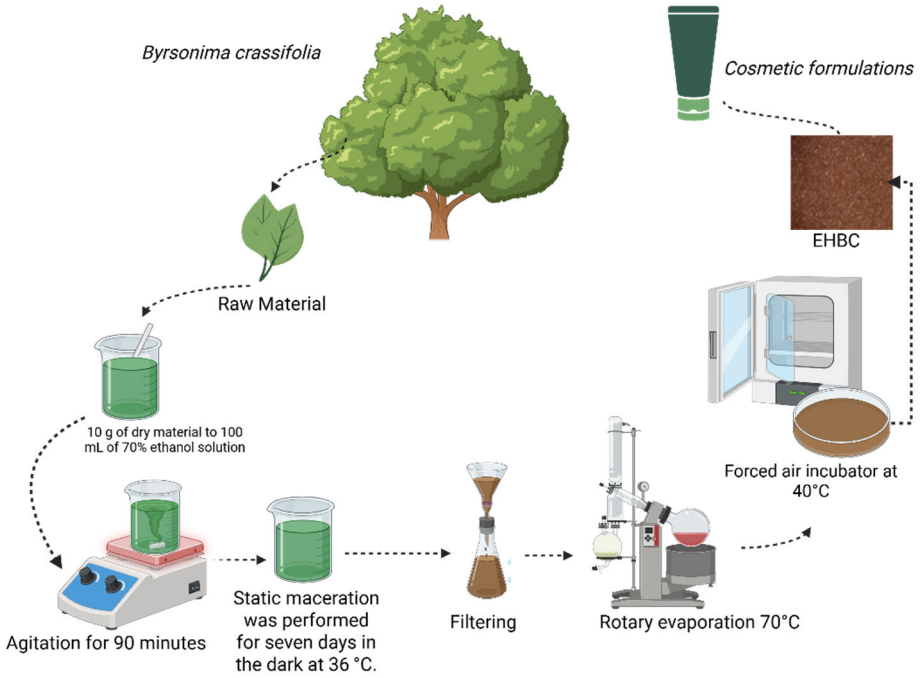


Figure 1. Method for obtaining HEBC.

2.3. Phytochemical Characterization of HEBC

Concentrations of 100, 200, 400, 800 and 1000 µg/mL were tested. The assays were conducted in triplicate.

2.3.1. Total Phenolic Compounds

The total phenolic content was determined using the Folin–Ciocalteu method, according to Khodaie et al. [10], with gallic acid as the standard. Extract samples, 1000 µL, were treated with 5 mL of distilled water, 250 µL of Folin–Ciocalteu reagent, and 1000 µL of 10% Na_2CO_3, and allowed to react for 1 h at 40 °C. Absorbance was measured using a UV–Vis spectrophotometer at 725 nm. The analytical curve for the gallic acid standard was: $y = 0.0092x - 0.0083$; $R^2 = 0.9982$.

2.3.2. Total Flavonoids

Flavonoid quantification was performed according to Zhishen et al. [11], with modifications by Khodaie et al. [10], with quercetin as the standard. Aliquots of the extract, 500 µL, were reacted with 1.5 mL of ethanol, 100 µL of 10% $AlCl_3$, 100 µL of CH_3COONa, and 2.8 mL of distilled water (final volume 5 mL) and kept in the dark for 30 min. Absorbance was measured using a spectrophotometer at 425 nm. The analytical curve for the quercetin standard was: $y = 0.0204x - 0.0009$; $R^2 = 0.9993$.

2.3.3. Total Condensed Tannins

Tannin condensing was performed through a colorimetric reaction with vanillin solution. The comparison standard was proanthocyanidin. In test tubes preheated to 30 °C for 30 min, 1.0 mL of the extract dissolved in ethyl alcohol, 2.5 mL of sulfuric acid (H_2SO_4) at 25% in ethyl alcohol (*v*/*v*), and 2.5 mL of vanillin 1% in ethyl alcohol (*w*/*v*) were added. The tubes were vortexed to homogenize and heated for 20 min at 30 °C in a water bath,

protected from light. Subsequently, the reading on a spectrophotometer was performed at 500 nm. The analytical curve for the proanthocyanidin standard was: $y = 0.0004x - 0.0034$; $R^2 = 0.9913$.

2.3.4. Fourier-Transform Infrared Spectroscopy (FTIR)

The FTIR analyses were performed at the Department of Life Sciences, Faculty of Science and Technology, University of Coimbra, Coimbra, Portugal. Spectra were acquired in attenuated total reflectance (ATR) mode within the mid-infrared region (400–4000 cm^{-1}) using a Bruker Optics Vertex 70 FTIR spectrometer purged with dry, CO_2-free air and equipped with a Bruker Platinum single-reflection diamond ATR accessory. A liquid-nitrogen-cooled mercury cadmium telluride (MCT) detector and a Ge beam splitter on a KBr substrate were employed for signal detection. Raw spectra were processed using Bruker Opus 8.1 software to (i) remove residual atmospheric H_2O and CO_2 contributions, and (ii) apply the frequency-dependent correction for ATR penetration depth (assuming an average refractive index of 1.25). Absorbance spectra were exported as text files and subsequently imported into MatLab (v. R2021b; MathWorks, Natick, MA, USA) for further chemometric preprocessing. Spectra were vector-normalized to unit length (2-Norm), baseline-corrected using the automatic weighted least squares algorithm (polynomial order = 2), and subjected to extended multiplicative scatter correction (EMSC) using the mean spectrum of the dataset as reference (polynomial order = 2). Chemometric relationships among the FTIR-ATR spectra were investigated in the fingerprint region (1800–800 cm^{-1}) via multivariate analysis using the Eigenvector PLS Toolbox (v. 9.0; Eigenvector Research, Wenatchee, WA, USA).

2.3.5. High-Performance Liquid Chromatography (HPLC) Analysis

Catechin was identified in the extract using high-performance liquid chromatography (HPLC). The mobile phase consisted of an aqueous solution of 0.1% formic acid (solvent A) and 0.1% formic acid in acetonitrile (solvent B). The solvent gradient was set as follows: from 0 to 3 min, 80% A; from 3 to 6 min, 80% to 65% A; from 6 to 11 min, 65% A; from 11 to 14 min, 65% to 30% A; from 14 to 18 min, 30% A; and finally, from 18 to 20 min, returning to 80% A. The flow rate was maintained at 1 mL/min, and the detector was set to a wavelength of 280 nm. Analyses were conducted on a Luna® C18 reverse-phase column (Phenomenex, 250 × 4.6 mm, 5 µm) at a temperature of 35 °C. The experiments utilized an online JASCO system equipped with a diode-array detector (JASCO, Easton, MD, USA). Peaks were identified by comparison with authentic catechin standards obtained from Sigma-Aldrich. A stock solution of catechin was prepared at a concentration of 10 mM in DMSO and then diluted in a water–ethanol mixture (50:50) to achieve a final concentration of 0.01 mM for HPLC analysis. The injection volume for the samples was 20 µL.

2.4. Cytotoxicity of HEBC

This assay was performed following a standard MTT cytotoxicity procedure adapted for NIH/3T3 fibroblasts. Cells were cultured in high-glucose DMEM supplemented with 10% FBS and 1% antibiotic-antimycotic solution at 37 °C in a humidified atmosphere with 5% CO_2. Cells were trypsinized at ~80% confluence, resuspended in supplemented DMEM, and counted with trypan blue to ensure ≥ 80% viability. The cell suspension was adjusted to 2.5×10^5 cells/mL and incubated overnight. Subsequently, 200 µL of treatments (100, 200, 400, 800 and 1600 µg/mL), diluted in supplemented DMEM (10% FBS) and filtered through a 0.22 µm filter, were seeded into each well. Treatments were performed in triplicate, and three separate plates were prepared for evaluation at 24, 48, and 72 h. Tween 80 (2% *v*/*v*) served as a positive control to confirm assay responsiveness, and serum-free DMEM was used as a negative control. After the incubation periods, 100 µL of MTT solution

(0.5 mg/mL in serum-free DMEM) was added to each well, excluding blanks, and plates were incubated for 4 h at 37 °C in 5% CO_2 to allow formation of formazan crystals. The medium was then removed, and 100 µL of sterile DMSO was added per well to solubilize the crystals. Plates were incubated for an additional 10 min, homogenized, and absorbance was measured at 560 nm using a microplate reader. The assays were conducted in triplicate.

2.5. Anti-Inflammatory Activity of HEBC

Concentrations of 100, 200, 400, and 800 µg/mL were tested. Cells alone served as the negative control, while dexamethasone at 100 µg/mL was used as the positive control. The assays were conducted in triplicate.

2.5.1. Phagocytosis Assay

The assay was conducted according to Libera et al. [12] and Azedo et al. [13], with modifications. The immortalized macrophage cell line RAW 264.7 (ATCC® TIB-71™) was employed in the study. Cells were seeded at a density of 2.5×10^5 cells per well in 96-well plates and allowed to adhere overnight in high-glucose DMEM® supplemented with 10% fetal bovine serum (FBS) and 1% penicillin–streptomycin. Cells were then stimulated with HEBC and dexamethasone at the specified concentrations and with zymosan (2×10^7 particles/mg. Following stimulation, cells were incubated for 2 h at 36 °C in a humidified atmosphere containing 5% CO_2. After fixation with 2.5% glutaraldehyde and staining with Wright's stain, phagocytosis was evaluated in 100 cells per coverslip using optical microscopy (400×).

2.5.2. Spreading Assay

The assay was performed according to Sampaio et al. [14]. The immortalized macrophage cell line RAW 264.7 (ATCC® TIB-71™) was used. Cells were seeded at a density of 2.5×10^5 cells per slide and allowed to adhere for 30 min. Subsequently, 10 µL of the HEBC concentrations were added in high-glucose DMEM®, while unstimulated cells served as controls. Slides were incubated for 1 h, then fixed with 2.5% glutaraldehyde, stained with Wright's stain, and analyzed by optical microscopy at 400× magnification. Macrophage spreading inhibition was determined by counting 100 cells per slide using optical microscopy (400×).

2.6. Antioxidant Activity of HEBC

Four concentrations of HEBC (100, 200, 400, and 800 µg/mL) were tested. The negative control consisted of the solvent (water), while quercetin at 0.2 mg/mL was used as the positive control. The assays were conducted in triplicate.

2.6.1. Lipid Peroxidation Inhibition Assay

Lipid peroxidation inhibition was evaluated using a 10% (*w*/*v*) egg yolk homogenate in 0.1 M phosphate buffer (pH 7.4), according to [15]. Samples were prepared by mixing 0.4 mL of extract with 4 mL of egg yolk homogenate and then inducing lipid peroxidation with 0.4 mL of $FeSO_4$ (0.17 M) for 30 min at 37 °C. Subsequently, 2 mL of 15% TCA and 2 mL of 0.67% TBA were added, and the mixture was heated at 95 °C for 60 min. Absorbance was measured at 532 nm, and the results were expressed as the percentage of lipid peroxidation inhibition.

2.6.2. DPPH Assay

Aliquots of 0.1 mL of the extract at different dilutions were mixed with 3.9 mL of DPPH solution (0.06 mM) prepared in absolute ethanol, with the control prepared using the solvent (water). Absorbance was measured at 517 nm, and the antioxidant activity was

expressed as the percentage of DPPH inhibition by the treatments. Subsequently, the IC_{50} value of the extract was determined [16].

2.7. Statistical Analysis

For the statistical analysis of the study, data from each of the assessments was employed using BioEstat 5.0 (Mamirauá Institute, Tefe, Brazil), and the results were discussed at the 5% level of significance. The data were subjected to one-way ANOVA, with treatment as an independent factor. Where appropriate, multiple comparisons were performed by a Tukey post hoc test.

3. Results

3.1. Phytochemical Screening of HEBC

Table 1 presents the phytochemical results obtained from the spectrophotometric analyses of HEBC, expressed as grams of standard equivalents per 100 g of dry extract.

Table 1. Mean ± SD of secondary metabolites present in HEBC.

Secondary Metabolites	g/100 g
Total Phenolic Compounds	13.83 ± 0.07 GAE
Flavonoids	1.34 ± 0.04 QE
Condensed tannins	11.30 ± 0.10 PE

GAE—gallic acid equivalent (g/100 g dry extract); QE—quercetin equivalent (g/100 g dry extract); PE—proanthocyanidin equivalent (g/100 g dry extract).

Chromatographic analysis of the HEBC revealed the presence of catechin. A peak corresponding to catechin was detected at a retention time of 10.1 ± 0.1 min, with high intensity, indicating a substantial concentration of this compound. The identity of catechin was confirmed by comparing its retention time with that of the standard (10.2 ± 0.1 min) (Figure 2A) and by evaluating the UV-Vis spectral similarity between the corresponding peaks.

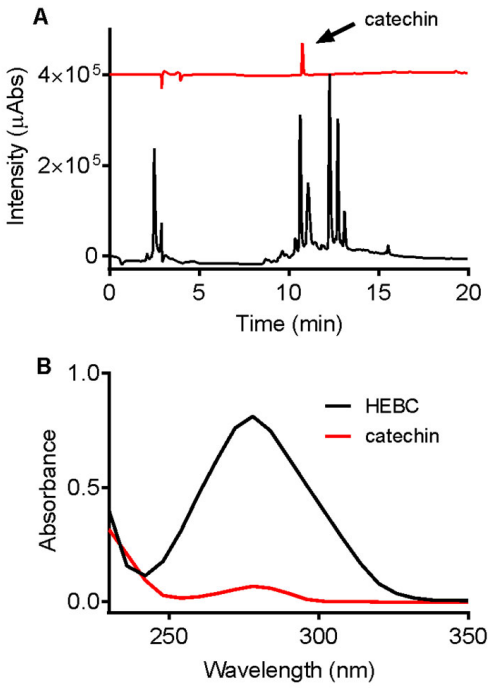


Figure 2. (**A**) Chromatogram of the HEBC (black) and catechin standard (red). (**B**) UV-Vis spectra of the peaks.

3.2. FTIR

The FTIR spectrum of HEBC (Figure 3) exhibits characteristic bands that indicate the presence of phenolic compounds, triterpenoids, and polysaccharides. The intense broadening observed at 3279 cm^{-1} is associated with O–H stretching of hydroxyl groups present in phenols, alcohols, and adsorbed water. The bands at 2933 cm^{-1} and 2854 cm^{-1} correspond to the asymmetric and symmetric stretching of C–H groups from aliphatic chains, typical of lipidic compounds and triterpenoids. The absorption at 1689 cm^{-1} indicates C=O stretching of strongly hydrogen-bonded carboxylic acids, whereas the peak at 1607 cm^{-1} is associated with aromatic ring vibrations (C=C) of phenolic compounds and possible lignin-like structures. The bands between 1519 and 1445 cm^{-1} confirm the presence of conjugated C=C bonds and CH_2 angular deformations, commonly found in secondary metabolites. The region between 1200 and 1034 cm^{-1} reveals C–O and C–C stretching modes characteristic of polysaccharides, pectins, and glycosides, supporting the polar nature of the extract. Finally, the absorptions at 871–768 cm^{-1} indicate out-of-plane C–H deformations in aromatic rings and possible contributions from triterpenes. Thus, the vibrational profile confirms that the murici extract is rich in phenolic and triterpenic substances, as well as structural sugars, in agreement with its phytochemical composition described in the literature.

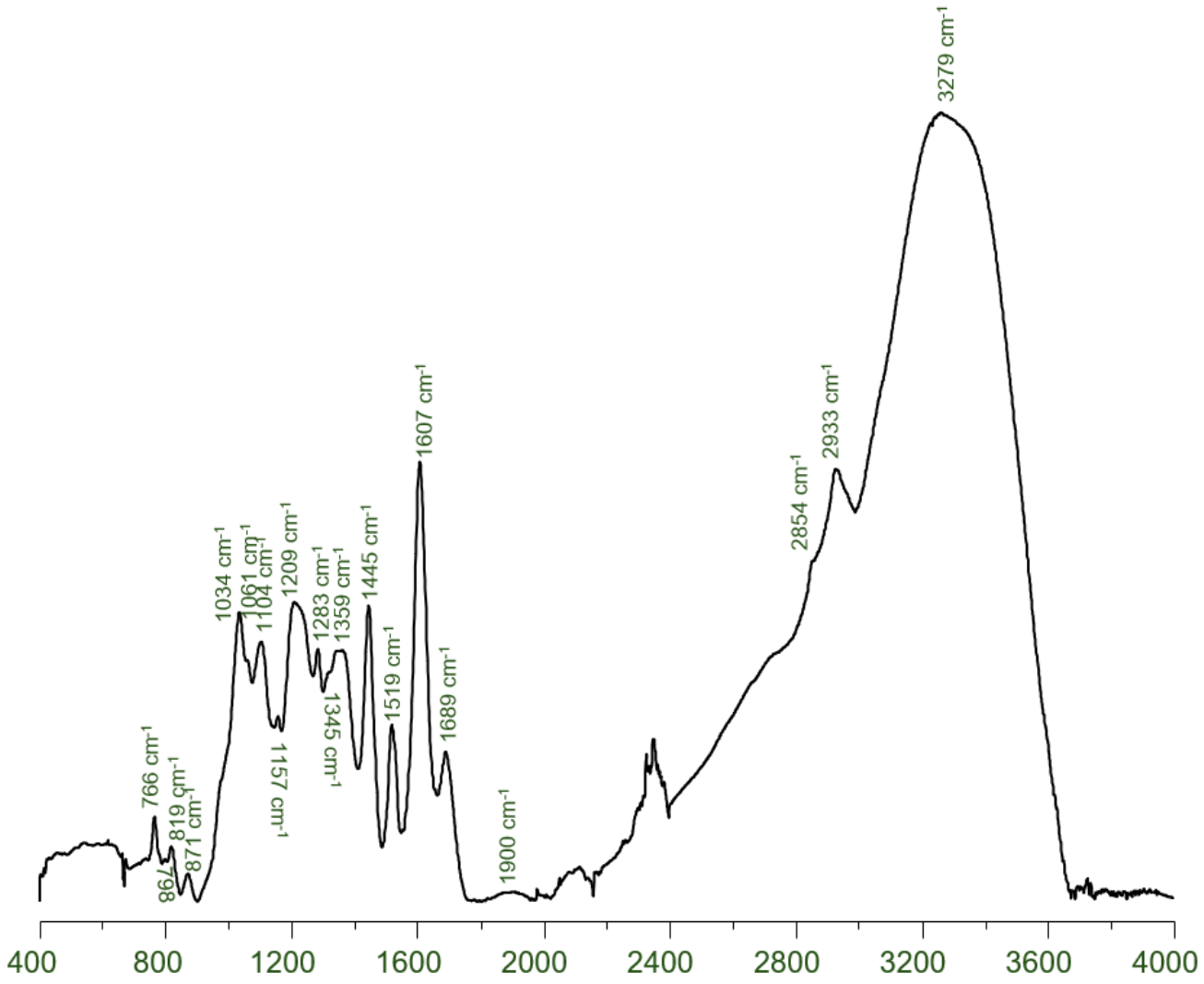


Figure 3. FTIR bands related to the HEBC.

3.3. Celular Viability of HEBC

The results in Figure 4 show, at all times analyzed, significant differences between treatments ($p < 0.05$). After 24 h, low concentrations of HEBC (100–400 µg/mL) maintained high viability in percentage, respectively, 97.92 ± 0.49, 88.27 ± 0.74 and 82.66 ± 0.82. At higher concentrations, 800–1600 µg/mL, viability decreased in percentage, respectively, 71.39 ± 0.08 and 60.46 ± 1.96. All concentrations were significantly higher than the positive control, 2% Tween 80 (6.05 ± 0.07%).

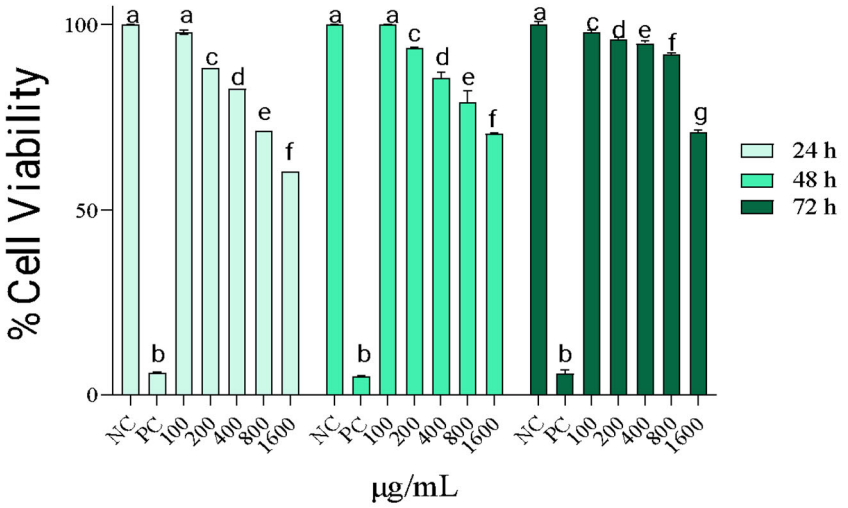


Figure 4. Mean ± SD of cell viability (%) in NIH 3T3 fibroblasts at 24, 48, and 72 h after treatment with the following: saline solution—negative control (NC); 2% Tween 80—positive control (PC); hydroalcoholic extract of *Byrsonima crassifolia* (HEBC) at 100, 200, 400, 800, and 1600 µg/mL. Identical letters indicate no statistically significant difference ($p > 0.05$) according to Tukey's test. Different letters indicate statistically significant differences ($p < 0.05$). Alphabetical order does not reflect the magnitude of the effect, only statistical differences.

At 48 h, the concentrations of HEBC (100–800 µg/mL) maintained high viability in percentage, respectively, 103.06 ± 0.08; 93.82 ± 0.08; 85.72 ± 1.39; and 80.87 ± 0.08. At the concentration of 1600 µg/mL, viability decreased in percentage to 70.69 ± 0.08. All concentrations were significantly higher than the positive control, 2% Tween 80 (5.13 ± 0.18%).

After 72 h, viability remained above 92% for concentrations up to 400 µg/mL. Thus, low concentrations of HEBC (100–800 µg/mL) maintained high viability in percentage, respectively, 98.49 ± 0.23, 96.48 ± 0.27, 95.89 ± 0.35 and 92.00 ± 049. Higher concentration (1600 µg/mL) showed greater reductions (71.10 ± 0.49).

3.4. Anti-Inflammatory Activity

Figure 5A presents the phagocytosis inhibition results. The negative control (NC) showed 0% inhibition, differing significantly from all treated groups ($p < 0.05$). The positive control (PC; dexamethasone 100 µg/mL) exhibited 95.05 ± 0.58% inhibition. HEBC produced a clear concentration-dependent response: 34.67 ± 3.86% (100 µg/mL), 55.98 ± 2.59% (200 µg/mL), 70.93 ± 1.47% (400 µg/mL), and 74.75 ± 1.71% (800 µg/mL). All concentrations differed significantly from the PC ($p < 0.05$). Comparative statistical analysis indicated that the difference between 400 and 800 µg/mL was not significant ($p > 0.05$), demonstrating a plateau in phagocytosis inhibition at higher concentrations, whereas concentrations from 100 to 400 µg/mL differed significantly from each other and from the NC ($p < 0.05$).

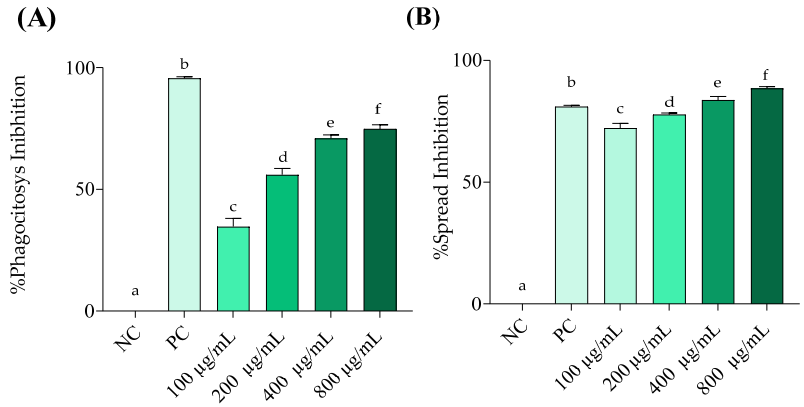


Figure 5. Mean ± SD of phagocytosis inhibition (**A**) and macrophage spreading inhibition (**B**) after treatment with saline (NC), dexamethasone at 100 µg/mL, and HEBC at 100, 200, 400, and 800 µg/mL. One-way ANOVA/Tukey. Identical letters indicate no significant difference ($p > 0.05$); different letters indicate significant differences ($p < 0.05$). Alphabetical order does not reflect effect magnitude, only statistical differences.

Figure 5B shows the macrophage spreading inhibition assay. NC exhibited 0% inhibition, while the PC showed 81.05 ± 0.53% inhibition. HEBC also produced dose-dependent inhibition: 72.29 ± 1.84% (100 µg/mL), 77.71 ± 0.70% (200 µg/mL), 83.73 ± 1.45% (400 µg/mL), and 88.55 ± 0.70% (800 µg/mL). The 800 µg/mL concentration resulted in greater inhibition than the PC ($p < 0.05$). Statistical comparisons revealed no significant difference between 400 and 800 µg/mL ($p > 0.05$), indicating a plateau in spreading inhibition similar to that observed in the phagocytosis assay. All concentrations from 100 to 400 µg/mL differed significantly from each other and from the NC ($p < 0.05$), reinforcing the concentration-dependent effect.

3.5. Antioxidant Activity

In the analysis of the in vitro antioxidant capacity of HEBC, the first assay performed was the lipid peroxidation (LPO) inhibition test (Figure 6A). The positive control (PC) exhibited 96.0 ± 0.00% antioxidant activity, while HEBC, 100–800 µg/mL, showed, in percentage, respectively, 76.65 ± 0.00, 79.10 ± 0.00, 84.19 ± 0.00 and 87.28 ± 0.00. All extract concentrations differed significantly from the negative control (NC) and the PC ($p < 0.05$). The half-maximal inhibitory concentration (IC_{50}) was 25–50 µg/mL.

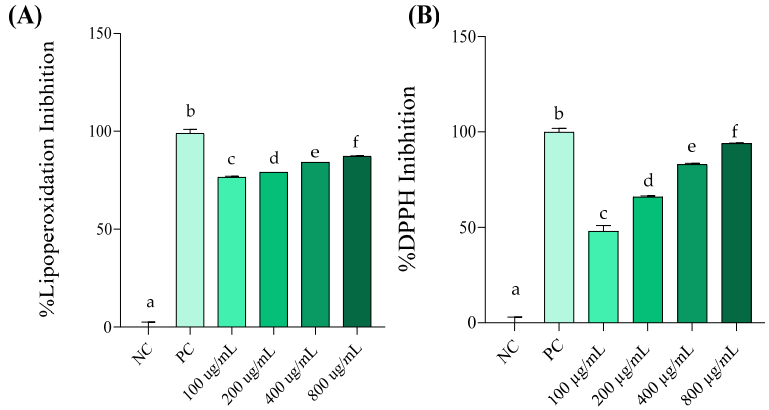


Figure 6. Mean ± SD of antioxidant activity in the lipid peroxidation (**A**) and DPPH (**B**) assays. Treatments: saline (NC), quercetin at 300 µg/mL, and HEBC at 100, 200, 400, and 800 µg/mL. One-way ANOVA/Tukey. Identical letters indicate no significant difference ($p > 0.05$); different letters indicate significant differences ($p < 0.05$). Alphabetical order does not reflect effect magnitude, only statistical differences.

Additionally, to evaluate the free radical scavenging potential of HEBC, the DPPH assay was performed (Figure 6B). In this assay, the positive control showed approximately 92.45 ± 0.00% antioxidant activity, while HEBC, 100–800 µg/mL, showed, in percentage, respectively, 48.55 ± 0.02, 66.49 ± 0.00, 89.71 ± 0.00 and 94.76 ± 0.00. All extract concentrations differed significantly from the negative control (NC) and the PC ($p < 0.05$). The 800 µg/mL concentration showed greater antioxidant activity than the PC ($p < 0.05$). The half-maximal inhibitory concentration (IC_{50}) was 103.20 µg/mL.

4. Discussion

The progressive increase in the global population has been associated with a higher prevalence of dermatological conditions, such as atopic dermatitis, psoriasis, acne, and premature skin aging, often linked to environmental factors, oxidative stress, and chronic inflammation [17,18]. At the same time, there is a growing demand for natural-origin cosmetic formulations, free from animal testing and enriched with sustainable bioactive compounds, a trend reflecting not only ethical concerns but also the adoption of the 3Rs principle (Replacement, Reduction, and Refinement), which guides the substitution, reduction, and refinement of animal use in research and development. In this context, the scope of this study was to investigate the hydroalcoholic plant extract of *Byrsonima crassifolia* (HEBC) for its therapeutic properties through in vitro assays, focusing on its potential as a candidate for dermocosmetic applications [2–22].

In the initial stage of this study, a phytochemical characterization of the phenolic compounds present in HEBC was performed, highlighting the importance of this class of secondary metabolites, widely recognized for their biological activities, including antioxidant, anti-inflammatory, and antimicrobial properties [7,23,24]. These compounds are essential for plants adaptation to adverse environmental stress and hold therapeutic relevance for humans, acting as modulators of complex pathophysiological processes. Spectrophotometric quantification revealed significant concentrations: 30.53 g of gallic acid equivalents for total phenols, 3.49 g of quercetin equivalents for flavonoids and 14.30 g of proanthocyanidin equivalents for condensed tannins, all per 100 g of dry extract.

Given the high concentration of condensed tannins in HEBC and considering that catechin is a precursor of this phenolic compound, the presence of catechin was analyzed and confirmed by a distinct peak detected at approximately 10 min of retention, characterized by intense absorption by chromatographic analysis (Figure 2). Literature reports indicate a potential presence of catechin in murici and corroborate that this secondary metabolite may be contributing to the antioxidant and anti-inflammatory activities observed in this study [25–30]. This is because catechins are well recognized for their antioxidant capacity and multiple health-promoting effects, including neutralizing free radicals and protecting against oxidative cellular damage [26]. Furthermore, in cosmetic applications, this phenolic compound is used for its ability to increase skin elasticity and attenuate inflammatory responses [6,9,27].

Current literature indicates that murici and its extracts, including leaves, fruits, and seeds, remain rich sources of phenolic compounds and exhibit high antioxidant and anti-inflammatory activities. Murici has been recognized as a valuable source of phytochemicals with multiple health benefits, including antioxidant, anti-inflammatory, antidiabetic, neuroprotective, and gastroprotective activities, as highlighted in a recent review [20]. The literature reports ethnopharmacological studies involving murici fruits, bark, and leaves using various extraction methods [28–33]. Pompeu et al. [32], for example, reported a total phenolic content of 3.69 g GAE/100 g for the hydroalcoholic leaf extract.

Aniceto et al. [34] found concentrations of 307.52 ± 19.73 mg GAE/100 g for total phenol and 174.87 ± 1.76 µg QE/g flavonoid content in the pulp of murici. In this analysis,

extract solutions containing the same proportion of the following solvents were used: (I) methanol, (II) 50% methanol, (III) 70% acetone and (IV) sequential. Subsequently, these solutions were added to the same phase flask with the addition of water. Sobrinho et al. [33], analyzing an extract obtained from murici leaves with three sequential solvent systems of increasing polarity—ethyl acetate, methanol and hydromethanolic solution (1:1 v:v)—found the presence of catechin at a concentration of 1.00 ± 0.40 mg CE/g, Comparatively, the concentrations obtained in the present study were higher than those reported in the literature, possibly due to the methodology employed, which used a more selective and efficient extraction system, maximizing metabolite recovery. Studies employing optimized extraction methods, such as ultrasound-assisted extraction, confirm that the phenolic compounds from *B. crassifolia* extracts have promising therapeutic potential, combining high antioxidant and anti-inflammatory activities with low cytotoxicity in human cells [34–37].

To confirm the high concentration of condensed tannins observed in the murici extract, as well as to establish a possible relationship with the pharmacological activities analyzed in this study, the presence of catechin, a precursor of condensed tannins, was analyzed by HPLC. Then, a detailed characterization of catechin was performed using high-performance liquid chromatography (HPLC) with a photodiode array detector at 280 nm. Notably, catechin was identified, a secondary metabolite that serves as the structural unit of condensed tannins. These tannins are polymers formed by catechin linkages, whose composition can directly influence bioactivity. Maldini et al. [38] identified, in a methanolic extract of *B. crassifolia* bark, six galloylated derivatives by HPLC—5-O-, 3-O-, 3,4-di-O-, 3,5-di-O-, and 3,4,5-tri-O-galloylquinic acids, in addition to (+)-epicatechin-3-gallate, (+)-catechin, and (+)-epicatechin—corroborating the results obtained with the leaves in the present study.

The infrared spectrum obtained for the HEBC revealed a vibrational profile characteristic of plant matrices rich in phenolic compounds, triterpenoids, and polysaccharides, confirming the chemical complexity previously described for the species [39–46]. The broad band centered at 3279 cm^{-1} reflects the O–H stretching of hydroxyl groups present in phenols and alcohols, indicating a strong presence of hydrogen bonding. The absorptions at approximately 2920 and 2854 cm^{-1} correspond to the asymmetric and symmetric C–H stretching of aliphatic chains ($\nu a/\nu s$ CH_2), consistent with triterpenic components and lipidic fractions [47–52]. The peak at 1689 cm^{-1} is attributed to the C=O stretching of highly hydrogen-bonded carboxylic acids, while the band at 1607 cm^{-1} is associated with aromatic ring vibrations (C=C), with possible overlap of stretching modes of carboxylate groups (COO^-) from polygalacturonates, typical of pectins.

In the 1200–1034 cm^{-1} region, multiple bands indicate C–O and C–C stretching related to polysaccharides, pectins, and glycosidic linkages, particularly those at 1047–1055 cm^{-1}, attributed to glycosidic C–O–C modes [41]. Absorptions between 834 and 777 cm^{-1} denote out-of-plane (C–H) deformations of aromatic rings, with contributions from syringyl-type motifs and $\rho(CH_2)$ vibrations associated with triterpenoids [39,40]. These findings are consistent with vibrational studies reported for plant extracts rich in polyphenols, in which similar bands were described by Martin et al. [52], Marques et al. [42], and Breda et al. [41], in agreement with consolidated vibrational literature and with the reference framework adopted in this study.

Additionally, previous studies on *B. crassifolia* reinforce the predominance of phenolic compounds and condensed tannins as major constituents of the genus [36], whose chemical features align with the bands observed in the present analysis. Thus, the spectroscopic profile of HEBC reflects the coexistence of phenolic and polysaccharide fractions, supporting the results obtained by HPLC and antioxidant assays, and confirming that the hydroalcoholic extraction was efficient in concentrating bioactive secondary metabolites with potential for sustainable dermocosmetic applications.

Following phytochemical characterization, the cytotoxicity of HEBC was evaluated in NIH 3T3 fibroblasts according to ISO 10993-5. According to this classification, which establishes guidelines for biocompatibility testing, a cytotoxicity value below 70% indicates a significant toxic potential or that the analyzed product is considered cytotoxic [39]. Cell viability was assessed using the MTT assay, a well-established method for measuring mitochondrial activity, reflecting cellular integrity and functionality [37,47]. In this context, the concentrations of 100, 200, and 400 μg/mL exhibited a wide safety margin, whereas 800 μg/mL showed 71.39% viability at 24 h, falling within the borderline range but still compliant with the guideline. These findings suggest that the extract has an adequate safety window for incorporation into dermocosmetic formulations, especially considering that the concentrations evaluated (100–800 μg/mL) reflect values that are technically relevant for the development of topical products. The cytotoxic evaluation demonstrated the absence of cytotoxicity of HEBC at concentrations of 100, 200 and 400 μg/mL at all times analyzed. After 72 h, all concentrations analyzed did not promote cytotoxicity.

These findings indicate that the extract is safe at concentrations up to 400 μg/mL. Miki et al. [37], analyzing the 60% ethanolic extract of murici pulp, reported no cytotoxic effects in healthy human cell lines (CCD 1059 Sk) at concentrations ranging from 0.25 to 5 mg/mL. However, the literature lacks toxicological studies on the leaves, highlighting the originality of the present work.

Despite the advances reported in the literature on *Byrsonima crassifolia*, available studies are mostly fragmented, addressing phytochemical, pharmacological, or toxicological aspects in isolation and generally using conventional organic solvents (such as methanol, acetone, or chloroform). To date, no studies have performed an integrated evaluation simultaneously encompassing phytochemical characterization, pharmacological potential (antioxidant and anti-inflammatory), and the toxicological profile of an extract obtained with a green, environmentally sustainable solvent. This gap underscores the relevance of the present study, which combines methodological innovation with the development of safer natural products aligned with the principles of green chemistry.

The anti-inflammatory effect of HEBC was investigated considering that inflammation is a key component of innate immunity, mediated by cells such as macrophages, which perform critical functions including spreading, cytoskeletal reorganization, migration to injury sites, and phagocytosis of pathogens and debris. These processes are accompanied by the release of pro-inflammatory cytokines, which regulate the immune response [49]. However, excessive activation can exacerbate tissue damage and contribute to chronic diseases. The spreading and phagocytosis assays showed that HEBC significantly reduced inflammatory activation at all tested concentrations. Previous studies support this potential: Orlandi et al. [49] observed a 49% reduction in edema with an aqueous leaf extract (300 mg/kg) in an animal model, while Maldini et al. [38] reported 77% inhibition with a topical chloroform extract (300 μg/cm^2).

The concentration-dependent effect observed in the macrophage phagocytosis and spreading assays indicates that the magnitude of the anti-inflammatory response increases proportionally with HEBC concentration. This behavior is consistent with the action of phenolic compounds, flavonoids, and tannins present in the extract, which modulate cellular activation and macrophage signaling, influencing processes such as cytoskeletal reorganization, migration, and phagocytosis [45]. Low extract concentrations may provide insufficient bioactive molecules to elicit a maximal effect, whereas intermediate or high concentrations enhance interactions with cellular receptors and enzymes, potentiating the inhibition of inflammatory responses. The similarity in effect between the 400 μg/mL and 800 μg/mL concentrations suggests that cellular targets may reach a saturation level, beyond which additional increases in dose do not result in greater efficacy. These findings

show that an intermediate concentration of 200 µg/mL induces a significant effect in this model. However, a concentration of 400 µg/mL presents similar efficacy to 800 µg/mL without compromising cell viability at all times analyzed. In order to complement the results obtained in the spreading and phagocytosis tests, future studies will be carried out to investigate molecular inflammatory markers (cytokine profiling, NO production, or Western blot for COX-2/iNOS expression).

Considering the relationship between inflammation and oxidative stress [45], the antioxidant activity of HEBC was also evaluated. Lipid peroxidation generates malondialdehyde (MDA), which can induce mutations and protein oxidation, contributing to inflammatory responses and pathologies [45]. The results obtained from the two analytical systems used to assess antioxidant activity demonstrated a robust antioxidant potential. In the DPPH assay, an IC_{50} value of 103.20 µg/mL was determined, indicating substantial free radical-scavenging capacity. A clear concentration-dependent response was observed, in which increasing concentrations resulted in progressively higher inhibition; notably, the concentration of 800 µg/mL achieved 87.28 ± 0.00% inhibition. In the lipid peroxidation assay, the IC_{50} was estimated to fall within the tested range (25–50 µg/mL), reflecting high efficiency in preventing oxidative damage even at low concentrations.

Previous studies have reported the antioxidant activity of different murici plant parts: Bejar et al. [53] identified quercetin as the main active compound (1.42 µmol TE/g of dry leaf, ORAC); Gordon et al. [36] observed that 5.26 g/L of fruit extract was required to inhibit 50% of peroxynitrite and hydroperoxyl radicals; Souza et al. [54] reported values ranging from 26.5 to 1621 µmol TE/g (ORAC and TRAP) for leaves, bark, and fruits.

In this context, considering its phytochemical profile, lack of cytotoxicity at doses up to 400 µg/mL, and notable anti-inflammatory and antioxidant activities, HEBC emerges as a promising candidate for incorporation into cosmetic formulations. The presence of phenolic compounds suggests potential for protecting the skin against inflammatory processes and oxidative damage, contributing to the delay of premature aging and the maintenance of skin integrity. Thus, the use of HEBC in dermocosmetic products may represent a sustainable strategy, adding value to Amazonian biodiversity and opening new avenues for the development of safe and effective natural cosmetics.

5. Conclusions

Based on the results obtained, the hydroalcoholic leaf extract of murici (HEBC) exhibited potent anti-inflammatory and antioxidant activities, without showing cytotoxicity at concentrations of 100, 200, and 400 µg/mL at all time points analyzed. These properties are likely associated with the high levels of phenolic compounds, particularly condensed tannins. Moreover, the hydroalcoholic extraction method, standardized in this study, proved more efficient than techniques reported in the literature using more toxic organic solvents. Thus, HEBC emerges as a promising candidate for the development of phytotherapeutics and for the enrichment of cosmetic formulations, contributing to the valorization and sustainable use of *Byrsonima crassifolia*.

Author Contributions: Conceptualization, L.d.S. and J.A.R.F.; methodology, J.A.R.F., F.Y.d.F., M.P.M.M., V.F.X. and G.J.-M.; software, L.T.S.d.C. and A.L.C.B.; writing—original draft preparation, K.A.A.-M. and N.A.Z.; visualization, J.T.R.-P.; project administration, L.d.S. All authors have read and agreed to the published version of the manuscript.

Funding: This research was funded by São Paulo Research Foundation (FAPESP), grant number 12/01751-7. J.A.R.F. was financially supported by the Coordination for the Improvement of Higher Education Personnel (CAPES—Brazil—888 87.827298/2023-00); L.T.S.d.C. was financially supported by the Coordination for the Improvement of Higher Education Personnel

(CAPES—Brazil—88887.817409-2023-00) and funded by the Portuguese Foundation for Science and Technology – UID/50006-2025.

Institutional Review Board Statement: This study did not involve human research; Institutional Review Board is not applicable.

Informed Consent Statement: This study did not involve human research; Informed Consent is not applicable.

Data Availability Statement: All data are contained in this article. The original contributions presented in this study are included in the article material. Further inquiries can be directed to the corresponding author(s).

Conflicts of Interest: The authors declare no conflicts of interest.

References

1. Kolb, L.; Ferrer-Bruker, S.J. Atopic Dermatitis. In *StatPearls*; StatPearls Publishing: Treasure Island, FL, USA, 2025.
2. Bertino, L.; Guarneri, F.; Cannavò, S.P.; Casciaro, M.; Pioggia, G.; Gangemi, S. Oxidative Stress and Atopic Dermatitis. *Antioxidants* **2020**, *9*, 196. [CrossRef] [PubMed]
3. Chanda, D.; Ha, H.; Lee, I.-K. Editorial: The Role of Oxidative Stress and Systemic Inflammation in Diabetes and Chronic Kidney Disease. *Front. Endocrinol.* **2023**, *14*, 1272525. [CrossRef] [PubMed]
4. Merecz-Sadowska, A.; Sitarek, P.; Kucharska, E.; Kowalczyk, T.; Zajdel, K.; Cegliński, T.; Zajdel, R. Antioxidant Properties of Plant-Derived Phenolic Compounds and Their Effect on Skin Fibroblast Cells. *Antioxidants* **2021**, *10*, 726. [CrossRef]
5. Olędzka, A.J.; Czerwińska, M.E. Role of Plant-Derived Compounds in the Molecular Pathways Related to Inflammation. *Int. J. Mol. Sci.* **2023**, *24*, 4666. [CrossRef]
6. Li, L.; Xie, H.; Wang, L.; Zhang, A.; Mou, X.; Lin, Y.; Ma, H.; Wang, Y.; Li, J.; Gao, J.; et al. The Efficacy and Safety of Combined Chinese Herbal Medicine and Western Medicine Therapy for COVID-19: A Systematic Review and Meta-Analysis. *Chin. Med.* **2022**, *17*, 77. [CrossRef]
7. Lima, T.P.B.; Coimbra, P.P.S.; da Silva Antonio, A.; Pereira, H.M.G.; da Silva, G.R.P.; da Veiga-Junior, V.F.; Silva, O.F.; Felzenszwalb, I.; Araujo-Lima, C.F.; Teodoro, A.J. Antioxidant Activity, Phytochemical Composition, and Antitumor Capacity of Amazonian Fruits Taperebá (*Spondias mombin*) and Murici (*Byrsonima crassifolia*). *Arch. Pharm.* **2025**, *358*, e2400758. [CrossRef]
8. Mariutti, L.R.B.; Rodrigues, E.; Mercadante, A.Z. Carotenoids from *Byrsonima crassifolia*: Identification, Quantification and In Vitro Scavenging Capacity Against Peroxyl Radicals. *J. Food Compos. Anal.* **2013**, *31*, 155–160. [CrossRef]
9. de la Cabeza Fernández, M.; Sánchez, M.; Caceres, A.; Iglesias, I.; Gómez-Serranillos, M.P. Neuropharmacological Effects in Animal Models and HPLC-Phytochemical Profiling of *Byrsonima crassifolia* (L.) Kunth Bark Extracts. *Molecules* **2023**, *28*, 764. [CrossRef]
10. Khodaie, L.; Bamdad, S.; Delazar, A.; Nazemiyeh, H. Antioxidant, Total Phenol and Flavonoid Contents of Two *Pedicularis* L. Species from Eastern Azerbaijan, Iran. *BioImpacts* **2012**, *2*, 43–57. [CrossRef] [PubMed]
11. Zhishen, J.; Mengcheng, T.; Jianming, W. The Determination of Flavonoid Contents in Mulberry and Their Scavenging Effects on Superoxide Radicals. *Food Chem.* **1999**, *64*, 555–559. [CrossRef]
12. Huang, D.; Ou, B.; Prior, R.L. The Chemistry behind Antioxidant Capacity Assays. *J. Agric. Food Chem.* **2005**, *53*, 1841–1856. [CrossRef]
13. Della Libera, A.M.M.P.; Birgel, E.H.; Kitamura, S.S.; Rosenfeld, A.M.F.; Mori, E.; Gomes, C.d.O.M.-S.; de Araújo, W.P. Macrófagos lácteos de búfalas hígidas: Avaliações da fagocitose, espraiamento e liberação de H_2O_2. *Braz. J. Vet. Res. Anim. Sci.* **2006**, *43*, 412–419. [CrossRef]
14. Azedo, M.R.; Blagitz, M.G.; Souza, F.N.; Benesi, F.J.; Della Libera, A.M.M.P. Avaliação funcional de monócitos de bovinos naturalmente infectados pelo vírus da leucose bovina. *Arq. Bras. Med. Vet. Zootec.* **2011**, *63*, 1131–1140. [CrossRef]
15. Sampaio, S.C.; Sousa-e-Silva, M.C.; Borelli, P.; Curi, R.; Cury, Y. *Crotalus durissus terrificus* Snake Venom Regulates Macrophage Metabolism and Function. *J. Leukoc. Biol.* **2001**, *70*, 551–558. [CrossRef] [PubMed]
16. Nascimento Júnior, B.J.; Santos, A.M.T.; Souza, A.T.; Santos, E.O.; Xavier, M.R.; Mendes, R.L.; Amorim, E.L.C. Estudo da ação da romã (*Punica granatum* L.) na cicatrização de úlceras induzidas por queimadura. *Rev. Bras. Plantas Med.* **2016**, *18*, 423–432. [CrossRef]
17. Garcia, E.J.; Oldoni, T.L.C.; de Alencar, S.M.; Reis, A.; Loguercio, A.D.; Grande, R.H.M. Antioxidant Activity by DPPH Assay of Potential Solutions to Be Applied on Bleached Teeth. *Braz. Dent. J.* **2012**, *23*, 22–27. [CrossRef] [PubMed]
18. Liu, J.; Martin, A.; Thatiparthi, A.; Wu, J.J. Association between Atopic Dermatitis and Osteoarthritis among US Adults in the 1999–2006 NHANES. *J. Eur. Acad. Dermatol. Venereol.* **2021**, *35*, e375–e377. [CrossRef]

19. Zuo, L.; Prather, E.R.; Stetskiv, M.; Garrison, D.E.; Meade, J.R.; Peace, T.I.; Zhou, T. Inflammaging and Oxidative Stress in Human Diseases: From Molecular Mechanisms to Novel Treatments. *Int. J. Mol. Sci.* **2019**, *20*, 4472. [CrossRef]
20. Martinez, R.M.; Cintra, A.C.; de Almeida, C.d.O.R.P.; Lima, T.P.B.; Moraes de Souza, I.; de Almeida, M.A.P.; Frankenfeld, S.P.; Cahuê, F.L.C.; de Queiroz Pereira Lopes, G.; Pinto, V.S.; et al. Bioactive Properties of Murici (*Byrsonima crassifolia*) and Bacuri (*Platonia insignis*) and Their Antioxidant and Anti-Inflammatory Effects in Rats. *J. Med. Food* **2025**, *28*, 478–489. [CrossRef]
21. Martins, A.M.; Marto, J.M. A Sustainable Life Cycle for Cosmetics: From Design and Development to Post-Use Phase. *Sustain. Chem. Pharm.* **2023**, *35*, 101178. [CrossRef]
22. Kiani, A.K.; Pheby, D.; Henehan, G.; Brown, R.; Sieving, P.; Sykora, P.; Marks, R.; Falsini, B.; Capodicasa, N.; Miertus, S.; et al. Ethical Considerations Regarding Animal Experimentation. *J. Prev. Med. Hyg.* **2022**, *63*, E255–E266. [CrossRef]
23. Revathy, M.S.; Elamathi, S.; Subrahmaniyan, K.; Rajarathinam, P.; Anandhi, P.; Devi, T.S.; Sivakumar, G. Therapeutic Potential of *Agave* spp. in Modern Healthcare: A Comprehensive Review. *Ann. Phytomed. Int. J.* **2024**, *13*, 365–375. [CrossRef]
24. Cioanca, O.; Lungu, I.-I.; Mita-Baciu, I.; Robu, S.; Burlec, A.F.; Hancianu, M.; Crivoi, F. Extraction and Purification of Catechins from Tea Leaves: An Overview of Methods, Advantages, and Disadvantages. *Separations* **2024**, *11*, 171. [CrossRef]
25. Sheng, Y.; Sun, Y.; Tang, Y.; Yu, Y.; Wang, J.; Zheng, F.; Li, Y.; Sun, Y. Catechins: Protective Mechanism of Antioxidant Stress in Atherosclerosis. *Front. Pharmacol.* **2023**, *14*, 1144878. [CrossRef]
26. Mokra, D.; Joskova, M.; Mokry, J. Therapeutic Effects of Green Tea Polyphenol (−)-Epigallocatechin-3-Gallate (EGCG) in Relation to Molecular Pathways Controlling Inflammation, Oxidative Stress, and Apoptosis. *Int. J. Mol. Sci.* **2022**, *24*, 340. [CrossRef] [PubMed]
27. Wangkarn, S.; Grudpan, K.; Khanongnuch, C.; Pattananandecha, T.; Apichai, S.; Saenjum, C. Development of HPLC Method for Catechins and Related Compounds Determination and Standardization in Miang (Traditional Lanna Fermented Tea Leaf in Northern Thailand). *Molecules* **2021**, *26*, 6052. [CrossRef]
28. de Souza, R.O.; Alves, G.A.D.; Forte, A.L.S.A.; Marquele-Oliveira, F.; da Silva, D.F.; Rogez, H.; Fonseca, M.J.V. *Byrsonima crassifolia* Extract and Fraction Prevent UVB-Induced Oxidative Stress in Keratinocytes Culture and Increase Antioxidant Activity on Skin. *Ind. Crops Prod.* **2017**, *108*, 485–494. [CrossRef]
29. Almeida, V.D.S.S.; Maranhão, M.F.C.; Vasconcelos, A.C.S.L.; Florentino, J.V.P.; Barros, W.C.; Rocha, R.B.; Carvalho, K.W.P. Pharmacological Properties of *Byrsonima crassifolia* (L.) Kunt. *Rev. Investig. Bioméd.* **2019**, *10*, 280.
30. Gellen, L.F.A.; Silva, E.H.C. Atividade antimicrobiana de extratos de raízes de *Byrsonima crassifolia*. *J. Bioenergy Food Sci.* **2016**, *3*, 63–71. [CrossRef]
31. Almeida, M.M.; Pires, F.C.S.; Silva, A.P.S.; Sousa, S.H.B.; Salaza, M.A.R.; Junior, R.N.C. Supercritical Fluid Extraction of Murici Leaves (*Byrsonima crassifolia*): Global Yield, Total Phenolic Compounds, Antioxidant Activity, and Linear Correlations. *Braz. J. Dev.* **2021**, *7*, 110898–110914. [CrossRef]
32. Andrade, B.S.; Matias, R.; Corrêa, B.O.; Oliveira, A.K.M.; Guidolin, D.G.F.; Roel, A.R. Phytochemistry, Antioxidant Potential and Antifungal Activity of *Byrsonima crassifolia* on Soil Phytopathogen Control. *Braz. J. Biol.* **2018**, *78*, 140–146. [CrossRef]
33. Pompeu, D.R.; Rogez, H.; Monteiro, K.M.; Tinti, S.V.; Carvalho, J.E. Capacidade antioxidante e triagem farmacológica de extratos brutos de folhas de *Byrsonima crassifolia* e de *Inga edulis*. *Acta Amazon.* **2012**, *42*, 165–172. [CrossRef]
34. Sobrinho, A.C.G.; Rogez, H.L.G.; Nascimento, V.H.A.; Teixeira, B.J.B.; Dias, A.L.S.; Souza, J.N.S. Determination of Bioactive Compounds and Scavenging Capacity of Free Radicals in *Byrsonima crassifolia* and *Inga edulis* Leaf Extracts. *Braz. J. Dev.* **2020**, *6*, 34954–34969. [CrossRef]
35. Aniceto, A.; Montenegro, J.; Cadena, R.S.; Teodoro, A.J. Physicochemical Characterization, Antioxidant Capacity, and Sensory Properties of Murici (*Byrsonima crassifolia* (L.) Kunth) and Taperebá (*Spondias mombin* L.) Beverages. *Molecules* **2021**, *26*, 332. [CrossRef] [PubMed]
36. Gordon, A.; Jungfer, E.; da Silva, B.A.; Maia, J.G.S.; Marx, F. Phenolic Constituents and Antioxidant Capacity of Four Underutilized Fruits from the Amazon Region. *J. Agric. Food Chem.* **2011**, *59*, 7688–7699. [CrossRef]
37. Sousa, S.B.; Lara Júnior, J.M.; Buarque, D.S. Optimization of the Extraction of Polyphenols and Antioxidant Capacity from *Byrsonima crassifolia* (L.) Kunth Fruit by Response Surface Methodology. In *Plant Physiological Aspects of Phenolic Compounds*; IntechOpen: London, UK, 2019. [CrossRef]
38. Miki, K.S.L.; Dresch, A.P.; Cavali, M.; da Silva, A.P.; Marafon, F.; Fogolari, O.; Mibielli, G.M.; Bagatini, M.D.; Bender, J.P. Influence of Drying Methods in the Ultrasound-Assisted Extraction of Bioactive Compounds from *Byrsonima crassifolia* to Evaluate Their Potential Antitumor Activity. *Food Humanity* **2024**, *2*, 100242. [CrossRef]
39. Maldini, M.; Sosa, S.; Montoro, P.; Giangaspero, A.; Balick, M.J.; Pizza, C.; Della Loggia, R. Screening of the Topical Anti-Inflammatory Activity of the Bark of *Acacia cornigera*, *Byrsonima crassifolia* Kunth, *Sweetia panamensis* Yakovlev and the Leaves of *Sphagneticola trilobata* Hitchcock. *J. Ethnopharmacol.* **2009**, *122*, 430–433. [CrossRef] [PubMed]
40. Gruber, S.; Nickel, A. Toxic or Not Toxic? The Specifications of the Standard ISO 10993-5 Are Not Explicit Enough to Yield Comparable Results in the Cytotoxicity Assessment of an Identical Medical Device. *Front. Med. Technol.* **2023**, *5*, 1195529. [CrossRef]

41. Ghasemi, M.; Turnbull, T.; Sebastian, S.; Kempson, I. The MTT Assay: Utility, Limitations, Pitfalls, and Interpretation in Bulk and Single-Cell Analysis. *Int. J. Mol. Sci.* **2021**, *22*, 12827. [CrossRef]
42. Madorran, E.; Ambrož, M.; Knez, J.; Sobočan, M. An Overview of the Current State of Cell Viability Assessment Methods Using OECD Classification. *Int. J. Mol. Sci.* **2024**, *26*, 220. [CrossRef]
43. Orlandi, L.; Vilela, F.C.; Santa-Cecília, F.V.; Dias, D.F.; Alves-da-Silva, G.; Giusti-Paiva, A. Anti-Inflammatory and Antinociceptive Effects of the Stem Bark of *Byrsonima intermedia* A. Juss. *J. Ethnopharmacol.* **2011**, *137*, 1469–1476. [CrossRef]
44. Gaschler, M.M.; Stockwell, B.R. Lipid Peroxidation in Cell Death. *Biochem. Biophys. Res. Commun.* **2017**, *482*, 419–425. [CrossRef] [PubMed]
45. Martin, D.; Marques, J.; Amado, A.M.; Barroca, M.J.; Moreira da Silva, A.; Batista de Carvalho, L.A.E.; Marques, M.P.M. Shedding Light into the Health-Beneficial Properties of *Corema album*—A Vibrational Spectroscopy Study. *J. Raman Spectrosc.* **2019**, *51*, 313–322. [CrossRef]
46. Martin, D.; Lopes, T.; Correia, S.; Canhoto, J.; Marques, M.P.M.; Batista de Carvalho, L.A.E. Nutraceutical Properties of Tamarillo Fruits: A Vibrational Study. *Spectrochim. Acta Part A Mol. Biomol. Spectrosc.* **2021**, *252*, 119501. [CrossRef] [PubMed]
47. Marques, J.; Martin, D.; Amado, A.M.; Lysenko, V.; Osorio, N.; Batista de Carvalho, L.A.E.; Marques, M.P.M.; Barroca, M.J.; Moreira da Silva, A. Novel Insights into *Corema album* Berries: Vibrational Profile and Biological Activity. *Plants* **2021**, *10*, 1761. [CrossRef]
48. da Costa, R.M.F.; Winters, A.; Hauck, B.; Martin, D.; Bosch, M.; Simister, R.; Gomez, L.D.; Batista de Carvalho, L.A.E.; Canhoto, J.M. Biorefining Potential of Wild-Grown *Arundo donax*, *Cortaderia selloana* and *Phragmites australis* and the Feasibility of White-Rot Fungi-Mediated Pretreatments. *Front. Plant Sci.* **2021**, *12*, 679966. [CrossRef] [PubMed]
49. Breda, C.A.; Morgado, D.L.; Assis, O.B.G.; Duarte, M.C.T. Processing and Characterization of Chitosan Films with Incorporation of Ethanolic Extract from "Pequi" Peels. *Macromol. Res.* **2017**, *25*, 1049–1056. [CrossRef]
50. Marques, M.P.; Martin, D.; Bosch, M.; Martins, J.; Biswal, A.K.; Zuzarte, M.; de Carvalho, L.B.; Canhoto, J.; da Costa, R. Unveiling the Compositional Remodelling of *Arbutus unedo* L. Fruits during Ripening. *Sci. Hortic.* **2022**, *303*, 111248. [CrossRef]
51. da Costa, R.M.F.; Bosch, M.; Simister, R.; Gomez, L.D.; Canhoto, J.M.; Batista de Carvalho, L.A.E. Valorisation Potential of Invasive *Acacia dealbata*, *A. longifolia* and *A. melanoxylon* from Land Clearings. *Molecules* **2022**, *27*, 7006. [CrossRef]
52. Landén, N.X.; Li, D.; Ståhle, M. Transition from Inflammation to Proliferation: A Critical Step During Wound Healing. *Cell Mol. Life Sci.* **2016**, *73*, 3861–3885. [CrossRef]
53. Bejar, E.; Amarquaye, A.; Che, C.; Malone, M.H.; Fong, H.H.S. Constituents of *Byrsonima crassifolia* and Their Spasmogenic Activity. *Int. J. Pharmacogn.* **1995**, *33*, 25–32. [CrossRef]
54. Souza, J.N.S.; Silva, E.M.; Loir, A.; Rees, J.-F.; Rogez, H.; Larondelle, Y. Antioxidant Capacity of Four Polyphenol-Rich Amazonian Plant Extracts: A Correlation Study Using Chemical and Biological In Vitro Assays. *Food Chem.* **2008**, *106*, 331–339. [CrossRef]

Disclaimer/Publisher's Note: The statements, opinions and data contained in all publications are solely those of the individual author(s) and contributor(s) and not of MDPI and/or the editor(s). MDPI and/or the editor(s) disclaim responsibility for any injury to people or property resulting from any ideas, methods, instructions or products referred to in the content.